JOURNAL OF PHYSICAL ORGANIC CHEMISTRY
J. Phys. Org. Chem. 2004; **17:** 602–614
Published online in Wiley InterScience (www.interscience.wiley.com). DOI: 10.1002/poc.778

Stereochemistry and secondary reactions in the irreversible inhibition of serine hydrolases by organophosphorus compounds†

Ildiko M. Kovach*

Department of Chemistry, The Catholic University of America, Washington, DC 20064, USA

Received 12 August 2003; revised 14 October 2003; accepted 15 October 2003

ABSTRACT: The stereoselectivity of phosphonylation of serine hydrolases by the ROR′P(O)X group of compounds is governed by the electronic properties of X, the size of RO groups, the active site milieu and the specific architecture of the active site of the serine hydrolase. For example, stereoselectivity in excess of 10^4 has been observed favoring the P(*S*) diastereomers of 2-(3,3-dimethylbutyl) methylphosphonofluoridate (soman) when phosphonylating acetylcholinesterases. Based on molecular dynamics simulations, this is attributable to specific binding of the pinacolyl group to Glu199, Trp84 and Phe331, which exert compression to effect F^- departure in the pentacoordinate transient (transition state or intermediate) of soman-inhibited cholinesterases. The pinacolyl group is not so well adapted at the acyl-binding site in the P(R) diastereomers reducing the efficiency of F^- expulsion. Serine hydrolase inactivation is often followed by secondary reactions. The electronic properties of ligands attached to P are decisive in whether C—O or P—O bond cleavage occurs in phosphonate diesters of serine hydrolases. Phenoxide ions leave readily with P—O cleavage from cholinesterases and chymotrypsin, the reaction resembling deacylation in the reaction of substrates. The architecture and electrostatic character of the active site govern the fate of a covalently attached phosphonyl fragment. Strong negative electrostatic and hydrophobic forces in the cholinesterases preferentially promote C—O bond cleavage with occasional methyl migration, whereas this route of dealkylation is nearly absent in phosphonate esters of serine proteases. Dealkylation in soman-inhibited cholinesterases is 10 orders of magnitude faster than in appropriate model reactions and occurs 10^4 times faster in the P(*S*) than in the P(*R*) diastereomers. It is driven by enzyme-facilitated methyl migration, occurring most likely concerted with C—O bond cleavage. Copyright © 2004 John Wiley & Sons, Ltd.

KEYWORDS: acetylcholinesterase inhibition; butyrylcholinesterase inhibition; serine protease inhibition; inhibition by soman; irreversible inhibition

INTRODUCTION

Scientific interest in the inhibition of cholinesterases (ChEs) by organophosphorus compounds has been sustained by the unusual efficiency of the unnatural, yet enzyme-catalyzed processes involved. Inhibition of other serine hydrolase enzymes by organophosphorus compounds also occurs, but with less severe physiological consequences than with ChEs. Inhibitors of serine hydrolases contain the central P═O (phosphyl)[1] functional group and enzyme inactivation results from nucleophilic attack at the P═O group in phosphates, phosphonates and phosphinates. Inhibition of serine hydrolase enzymes with organophosphorus compounds has vast chemical, pharmacological and medical implications that have unfortunately not been reviewed. Such a review certainly extends far beyond the scope of the perspective offered here. The inhibition of serine hydrolases by organophosphorus compounds is generally considered in three distinct phases: phosphylation, dephosphylation and aging or dealkylation or dearylation.[2] As all these reactions exploit the enzyme's acid–base catalytic apparatus, the pioneering work of William W. Jencks on the fundamental thermodynamic principles governing acid–base catalysis and proton transfer, especially by serine hydrolase enzymes, are most relevant and provide the inspiration and framework for this review.[3]

A paradigm of organophosphorus inhibitors of serine hydrolases is 2-(3,3-dimethylbutyl) methylphosphonofluoridate (soman). A chief characteristic of the soman-inhibited ChEs is the resilience to enzyme-catalyzed dephosphonylation due to the onset of competing and

**Correspondence to:* I. M. Kovach, Department of Chemistry, The Catholic University of America, Washington, DC 20064, USA.
E-mail: kovach@cua.edu
Contract/grant sponsor: USAMRICD; *Contract/grant number:* DAMD17-C-98-8021.
Contract/grant sponsor: USAMRICD; *Contract/grant number:* DAAH04-96-C-0086.
Contract/grant sponsor: NSF; *Contract/grant number:* MCB9205927.
Contract/grant sponsor: NIH; *Contract/grant number:* 1 F33 AG05742–01.
†Selected paper part of a special issue entitled 'Biological Applications of Physical Organic Chemistry dedicated to Prof. William P. Jencks'.

rapid dealkylation.[2,4–28] Both the inactivation and the ensuing aging reaction, loss of the pinacolyl group in the phosphonyl fragment, occur with the participation of acid–base catalysis.[2–5,8,10–13,15,16,26] ChE-promoted dealkylation is at least ten orders of magnitude faster than the non-enzymic equivalent.[11,12] Due to the great efficiency of the chemical transformations and the rapid route of entry into vertebrates, soman is one the most potent nerve agents known. Application of soman as a nerve gas against civilian or military populations further necessitated efforts towards a full elucidation of the mechanisms of each phase of the inhibition process.

HOW DOES PHOSPHYLATION COMPARE WITH ACYLATION OF SERINE HYDROLASES?

Phosphylation is avidly catalyzed by the enzymes and occurs with great efficiency with good leaving groups.[2,7] The adducts formed are considered analogs for the tetrahedral intermediate in deacylation of the enzymes by substrates. There is, however, greater charge separation and polarization in phosphylated adducts than in acyl-Ser enzyme transients,[29] which confers unique stabilizing interactions between active-site residues and phosphonate fragment resulting in irreversible inhibition. Mechanistic studies of the early phases of the inactivation of ChEs by soman were carried out in this laboratory and the results were reported in a series of papers.[4,5,7,30–36] A feature article[2] summed up the main conclusions in which the underlying reason for the irreversible inhibition was proposed to be differences in the stereochemical arrangement at the transition states of reactions of the natural substrate and the organophosphorus compounds. The stereochemical relationship between ligands in pentacoordinate phosphonyl transients and the His of the catalytic triad, discerned from Scheme 1, disfavors the proton transfer sequence requisite in acylation and deacylation of the catalytic Ser in serine hydrolases.[37–39] Leaving groups tend to depart from the axial position in the trigonal pipyramid, distant from the protonated His, but groups with a low p*K* can leave without protonation. The consequence is that the catalytic His remains protonated after leaving-group departure, because it is sequestered from proton acceptors, and *the acid–base apparatus is thus impaired*: this might be termed mechanism-based inhibition. A significant implication of this mechanism is the lack of general base catalysis of the hydrolysis of the phosphonylated enzyme adducts and, thus, a near absence of dephosphonylation. Subsequent work with the Gly117His mutants of butyrylcholinesterase (BChE) showed that a strategically placed His can restore the general base catalytic feature of the enzyme and, thus, enhance the rate of dephosphonylation from a number of adducts.[40] However, a conformational change occurring during phosphonylation has also been proposed and

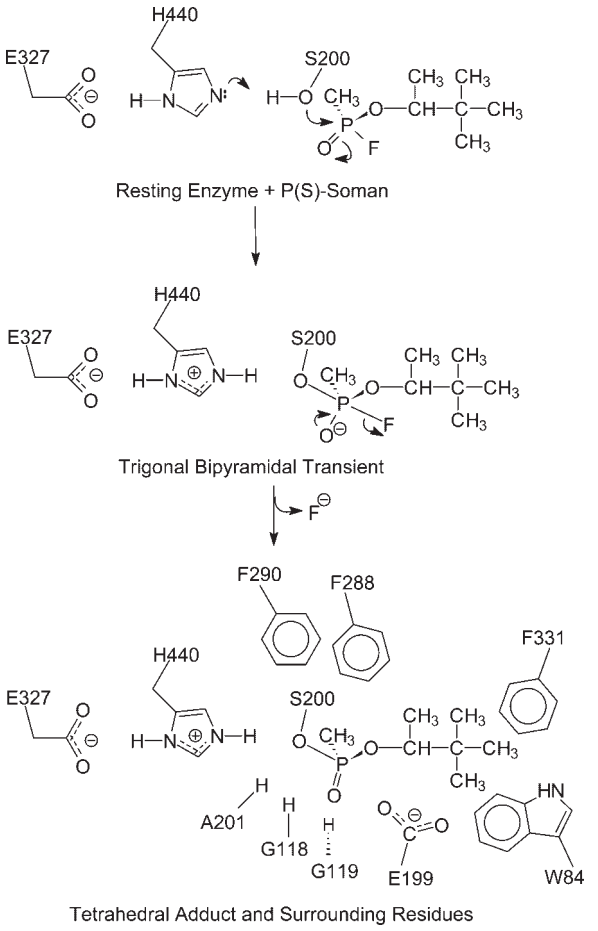

Scheme 1

cannot be excluded from preventing dephosphylation.[18] The earlier paper[2] also speculated on the need for a catalytic triad involving a carboxylic acid and the presence of a tryptophan residue in the binding region. Tryptophan residues are critical components of binding pockets, serine proteases also have a conserved Trp (215 in pancreatic enzymes) to form the wall of the specificity pocket.[35] The residues Ser200, His440, Glu327 and Trp84 were in fact found in the crystal structure of *Torpedo californica* (*Tc*) acetylcholinesterase (AChE),[41] also shown in Scheme 1. A tripartide oxyanion hole, different from serine proteases and without H-bond donation by the NH of the catalytic serine, provides stabilization to transition states and phosphyl centers in inhibitors.[41,42] Another conserved residue in serine proteases, Asp194, which is crucial in zymogen activation, also has a counterpart in ChEs, it is Glu199 in *Tc* AChE (Scheme 1). However, the side-chain conformation of Glu199 reveals its completely different role in ChEs, it is more similar to homologous lipases.[43] Immediately after the x-ray coordinates of *Tc* AChE became available, computational chemistry was used to identify the active-site residues that may promote the reaction at each stage.[4,5,8–10,44]

It has been our hypothesis that hydrolysis of the phosphonate fragment from the enzymes is hampered

by interference with the normal acid base-catalytic function of the catalytic triad (Asp/Glu, His, Ser) of the enzymes. We tested this hypothesis by studying the enantioselectivity and dynamics of phosphonylation, and the nature of interactions leading to dephosphonylation versus secondary reactions leading to the formation of anionic monoester adducts.

ENANTIOSELECTIVITY OF PHOSPHONYLATION IN SERINE HYDROLASES

The enantioselectivity of phosphonylation with compounds of the general structure ROR′P(O)X of ChE is for the enantiomer with P(*S*) configuration: enantioselectivity is the greatest when X = F among F, Cl and 4-nitrophenol.[45] The effect of R in the side-chain is also the greatest when X = F and R is branched with resemblance to the choline side-chain of the natural substrate: the best example is soman. With increasing size of R, however, the mode of binding and the preference for the P(*S*) enantiomer may change.[42] For comparison, chymotrypsin also has preference for the P(*S*) enantiomers of the same inhibitors, but with much smaller enantioselectivity than ChEs. In contrast to chymotrypsin, the preference is for P(*R*) in trypsin and subtilisin, if R is sizable. In general, the architecture and electrostatic character at the active site of an enzyme are decisive factors in enantioselectivity.

Inactivation of ChEs with the diastereomers of soman

Racemic soman is a mixture of four diastereomers due to the presence of one chiral center at the P atom and one at the Cα atom of the pinacolyl group. Inhibition studies with stereoisomers of soman have shown that the enantioselectivity of AChEs for soman is $>10^4$ favoring the P(*S*) configuration;[14,16,27,45] it is <500 for BChEs.[27] We have addressed the root causes of this enantioselectivity by model calculations using pentacoordinate adducts of the P(*S*)C(*S*)- and P(*R*)C(*S*)-soman-inhibited adducts of *Tc* AChE before the currently available x-ray structures of tetracoordinate phosphyl adducts of ChEs were published.[8–10] An initial calculation[8] with models generated using geometry-optimized selected conformations already gave insight into the origins of stereoselectivity in phosphonylation of AChE by P(*S*)C(*S*)- versus P(*R*)C(*S*)-soman. A rationale was also given based on the calculations for the reported[14,45] small selectivity for chiral differences in Cα. Nevertheless, this approach did not lead to viable conformations of the P(*R*)-soman inhibited AChE adducts.[8] The calculation was rectified a year later,[9] when it predicted successfully the conformation of the tetracoordinate P(*R*)-soman-inhibited AChE, which was later found by x-ray in the diisopropylphosphate-inhibited AChE.[28] The breakthrough came with molecular dynamics, allowing for greater torsional barrier crossing, some skeletal movement and a torsional adjustment of the indole side chain in Trp233 in the vicinity of the acyl-binding site. These were the necessary motions to accommodate the pinacolyl group in the P(*R*) enantiomer of soman at the acyl-binding site of AChE. Other acyl-binding-site residues, such as Phe290 and Phe288, were found to be very mobile, implying no significant obstacle to placing the pinacolyl group into the acyl pocket. These models are in remarkable agreement with findings of later kinetic studies of inhibition of recombinant (r) Hu AChE mutants by P(*R*) diastereomers of soman.[27] The models proposed for the structure of the tetracoordinate P(*S*)C(*S*)- and P(*R*)C(*S*)-soman-inhibited r Hu AChE have essentially the same binding elements in Ref. 27 as our models do.[9,10] Regrettably, our correct model remained unnoticed, while the incorrect model was cited.[27]

Insight into the structural basis of selectivity

Insight was gleaned from simulations with the first pentacoordinate phosphonate transients formed immediately after nucleophilic attack by Ser200 on P(*S*)C(*S*)- and P(*R*)C(*S*)-soman diastereomers. The phosphonyl oxygen maintained the H-bonding interaction with the three H-donors of the oxyanion hole in both diastereomers and through the tetracoordinate adducts. The nucleophile and the F^- leaving group were placed in the axial positions for an in-line attack. Minor movements of the pinacolyl group were observed in the pentacoordinate P(*S*)C(*S*)-soman–AChE adduct, towards an optimal overlap with Trp84 (Fig. 5 in Ref. 9). Apparently, this interaction exerts a compression from the equatorial plane of the trigonal bipyramid that can affect rapid elimination of the F^- in the pentacoordinate transient. Protonation of F^- is probably achieved by a proton donor other than $HisH^+440$, which is not near the F^- leaving group. Even with small adjustments of the backbone, the crowded active site showed other significant interactions between active-site residues and phosphonate fragment in the P(*S*)C(*S*)-soman adducts of AChE. These included shortening of the H-bonding distance to <2.65 Å between $HisH^+440$ Nδ and Glu327 Oε and somewhat longer between $HisH^+440$ NδH and Glu199 Oε. Two potential forces were identified for efficient expulsion of F^- in P(*S*)C(*S*)-soman adducts of AChE, the steric strain caused by binding the pinacolyl moiety at Trp84 and the electrostatic 'push' from Glu199 on one side of the phosphonyl fragment. The importance of the two residues can be assessed from results of kinetic studies with Trp86Ala, Glu202Ala, Glu202Gln and Glu202Asp mutants of ChEs. Glu199 mutations in *Tc* AChE were studied first[42] and showed significant rate reductions with Glu199Ala and

Glu199Gln mutants in acylation (50-fold), carbamoylation (3–21-fold) and phosphonylation (50–260-fold) at pH 7.0. The rate reductions with Glu199Asp mutations were always much smaller, which raised the specter of an electrostatic role of Glu199 in AChE function.[42] However, observations under different experimental conditions and with different species of AChE, were interpreted otherwise. Rate reductions of phosphonylation by racemic soman were small, 20–30-fold, with the Glu202Gln and Trp86Ala mutants of r Hu AChE[19,20] at pH 8.0, which also led to the belief[22,24,27] that pinacolyl binding to Trp86 in r Hu AChE is not a major factor in phosphonylation. In sharp contrast, phosphonylation is surprisingly slower, 263–685-fold, in the Trp82Ala mutants of Hu BChE than in the native enzyme at pH 7.5 and 25.0 °C.[26] Removal of the indole ring of Trp82 results in a great reduction in binding of the pinacolyl group of P(*S*) diastereomers of soman in r Hu BChE. The amount of data obtained with mutants is staggering in the cholinesterase field, but few effects on kinetics and mechanisms have been properly explored. Since it is impossible to dissect correctly the effects of replacement of a functional group or changing the length of a side-chain from a single datum, the conclusions drawn from single measurements under one set of conditions should be interpreted with great precaution. Millard *et al.*[40b] demonstrated with double mutants of Hu BChE that the effects of mutations are cooperative for phosphonylation by P(*S*)C(*S*) diastereomers of soman but additive for phosphonylation by P(*S*)C(*R*) diastereomers.

Simulations of the pentacoordinate P(*R*)C(*S*)-soman-inhibited AChE diastereomer were started from three different conformations, and two of these converged on the structure in which the pinacolyl-binding site was created at the acyl-binding pocket with some adjustment as described above (Fig. 6 in Ref. 9). The accommodation of the pinacolyl group at the indole ring of Trp84 is favorable over that in the acyl-binding pocket by $\sim 5.0\,\text{kcal mol}^{-1}$ ($1\,\text{kcal} = 4.184\,\text{kJ}$) in the minimized structures, which is comfortably close to the $5.6\,\text{kcal mol}^{-1}$ energy difference calculated from inhibition rate constants for the phosphonylation of AChEs by diastereomers of soman.[9]

Simulations

Simulations were also performed with the covalently modified tetracoordinate adducts of AChE with the two diastereomers of soman. Probably the most significant insight obtained from these simulations was that the H-bonding distance between $HisH^+440$ NδH and Glu199 Oε shrinks the most in the P(*S*)C(*S*)-soman-inhibited adducts of AChE to 2.6–2.8 from 4–4.2 Å in the corresponding pentacoordinate adduct and native enzyme, indicating a significant role of Glu199 in the secondary, dealkylation, reaction. The H-bonding partners $HisH^+440$ and Glu199 occupy a plane over the pinacolyl group in the covalently-bound phosphonate fragment and are poised to engage in interactions with the separating fragments around the C–O bond (see below).

In general, the active site was more crowded in the soman-inhibited adducts than in the structures of the tetrahedral intermediate formed after acetylation of AChE: the distances between $HisH^+440$ Nδ and either Glu327 Oε or Glu199 Oε hovered between 2.6 and 3.0 Å in 200 ps simulations of the P(*S*)C(*S*)-soman-inhibited AChE adduct.[9,10] It is then prudent to state that observations with phosphyl adducts of AChE may not be directly applicable to catalysis of the natural reaction.[8–10]

Chiral center in Cα

The chiral center in Cα has less impact on phosphonylation of ChEs; P(*S*)C(*S*)-soman is a slightly more potent inhibitor than the P(*S*)C(*R*) diastereomer. Bovine erythrocyte AChE exhibited a 6-fold difference in the bimolecular rate constants for the two P(*S*) diastereomers as compared with a 1.6-fold difference observed for electric eel (Ee) AChE.[16,45] The stereoselectivity is small in the wild-type mouse (Mo) AChE,[23] r Hu AChE[27] and ~ 7 in r Hu BChE,[26,40] but increases in the reaction involving some mutants. Replacement of Glu197, the acidic residue preceding the active-site Ser198 in Hu BChE, by Asp or Asn results in 4.5- and 11.8- fold decreases in the rate of phosphonylation with P(*S*)C(*S*)-soman compared with 6.5- and 47-fold decreases with P(*S*)C(*R*)-soman at pH 7.5 and 25.0 °C.[26] Glu202Gln, Glu450Ala and Tyr133Phe mutations in r Hu AChE cause 52–125- and 240–890-fold decrease in reactivity toward P(*S*)C(*S*)- and P(*S*)C(*R*)-soman at pH 8.0 and 27.0 °C, respectively.[27] These results show that the loss of charge on Glu202/197 decreases the reactivity of soman for mutant Hu AChE and BChE and significantly more so with the P(*S*)C(*R*) diastereomer, possibly owing to a greater loss of the electrostatic push of F^- by Glu202/197, due to the substitution in Cα. The effect of this mutation is greater in Hu AChE and Hu BChE than in Mo AChE.[23] Interestingly, mutations in Glu450 and Tyr133 in Hu AChE caused slightly larger rate reduction than the Glu202Gln mutation. It was proposed that the three residues (199, 450 and 130 in *Tc* AChE) form an H-bonding network,[27,41] inferred from the similar structure of *Geotrichium* lipase.[42,43] Mutations in the three residues then have been interpreted in terms of disruption of the H-bonding network. If there is such a H-bonding network in the resting state of AChE, it should be very sensitive to ionization states of neighboring residues that can compete for H-bonding as either the pH or the protein conformation changes. For example, protonated His440 interacts with Glu199, Trp84 seems to interact with Tyr130 and Glu443 readily interacts with neighboring residues in long molecular dynamics simulations (see

below). In fact, the Tyr133Ala mutation caused a 4550–17 400-fold reduction in the rate of phosphonylation of r Hu AChE by the P(*S*) diastereomers of soman. The authors invoked a major conformational change affecting the orientation of Trp86, which in turn blocks the active site.[27]

THE FATE OF COVALENTLY ATTACHED PHOSPHONYL FRAGMENTS IN SERINE HYDROLASES[46,47]

We characterized the properties of the transition states for these secondary reactions with C—O[11,12,26,46–48] and P—O[49] bond cleavage by pH dependence, the use of isotope effects,[11,12,26,46–49] thermodynamic parameters[11] and computational techniques.[4,6,8–10,44] Catalytic residues that induce C—O bond cleavage have been identified especially in the ChEs.[11,12,20–28,42,44,46–48] We also defined the molecular features that promote P—O bond breaking in chymotrypsin covalently modified with 4-nitrophenyl methyl- and propylphosphonate.[49]

Cholinesterases

The first presentation of the structural model explained dealkylation in soman-inhibited ChEs by a push–pull mechanism involving $HisH^+440$, Glu199 and Trp84 residues.[4] His440 was fully protonated in the model to correspond to the neutron-diffraction structure of the monoisopropylphosphate adduct of trypsin[50] and results of other NMR studies.[51–54] This model indicated that one of the methyl groups of the pinacolyl residue of soman binds to Trp84, while at least one methyl group and the C backbone are in the vicinity of Glu199. An identical mode of interaction between methyl groups of *m*-(*N*,*N*,*N*-trimethylammonio)trifluoroacetophenone (TMTFA) in the transition state analog inhibitor and Trp84 and Glu199 was later found by x-ray crystallography of the inhibited *Tc* AChE.[55]

pH dependence of the dealkylation reaction in soman-inhibited ChEs. An important test of the mechanism has been the pH dependence of the dealkylation reaction in soman-inactivated wild-type AChEs.[11,12,26,46–48]

The dependence on pH, of the rate constants for dealkylation in Ee, fetal bovine serum (FBS), r Mo AChE and r Hu BChE, and mutants of the latter two, inactivated with P(*S*)C(*S*)- and P(*S*)C(*R*)-soman, are bell-shaped and consistent with the push–pull mechanism. A peculiar characteristic of the pH profiles is the very steep rise in the rate of aging with pH between 3.5 and 5.0 as displayed in Fig. 1. A similar observation has been reported by Selwood *et al.* on reactions of Ee AChE with substrates that have large acyl groups.[56] Best-fit parameters for the asymmetric bell-shaped curves, Fig. 1 for the adducts of wild-type Ee and FBS and Fig. 2(A) for

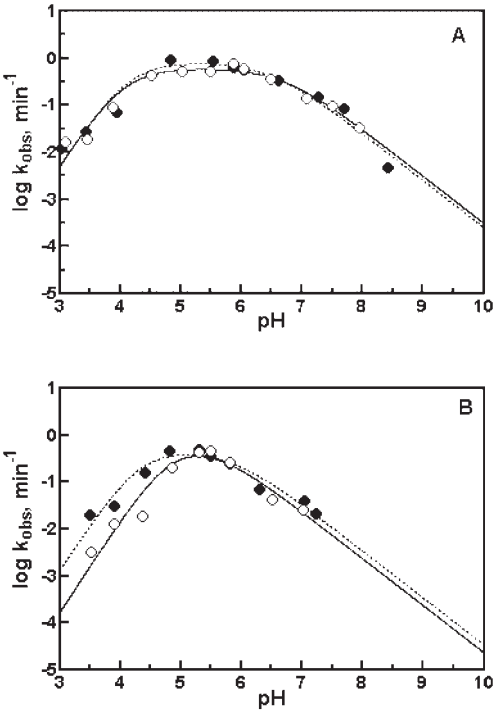

Figure 1. (A) Log *k* of dealkylation versus pH profiles for Ee AChE inhibited with P(*S*)C(*R*)-soman (○) and P(*S*)C(*S*) soman (●). (B) Log*k* of dealkylation versus pH profiles for FBS AChE inhibited with P(*S*)C(*R*)-soman (○) and P(*S*)C(*S*)-soman (●)

Mo AChE, are $pK_1 = pK_2 = 4.0$–4.9 and $pK_3 = 5.2$–6.6. The calculated p*K*s, limiting rate constants and solvent isotope effects are given for a number of ChEs in Table 1.

These p*K*s are consistent with the involvement of two carboxylic acids, possibly Glu199/202 and either Glu327/334 or Glu443/450, and $His440/447H^+$ in the dealkylation of AChE. Glu202Gln MoAChE inactivated

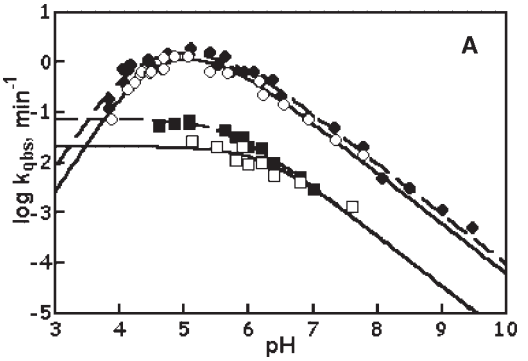

Figure 2. (A) Log *k* of dealkylation versus pH profiles for r Mo AChE inhibited with P(*S*)C(*R*)-soman (○) and P(*S*)C(*S*)-soman (●); for the E202Q mutant of Mo AChE inhibited with P(*S*)C(*R*)-soman (□) and P(*S*)C(*S*)-soman (■). (B) Log *k* of dealkylation versus pH profiles for r Hu BChE inhibited with P(*S*)C(*R*)-soman (○) and P(*S*)C(*S*)-soman (●); for the E197Q mutant of Hu BChE inhibited with P(*S*)C(*R*)-soman (□) and P(*S*)C(*S*)-soman (■); for the E197D mutant of Hu BChE inhibited with P(*S*)C(*R*)-soman (△) and P(*S*)C(*S*)-soman (▲); for the W82A mutant of Hu BChE inhibited with P(*S*)C(*R*)-soman (▽) and P(*S*)C(*S*)-soman (▼)

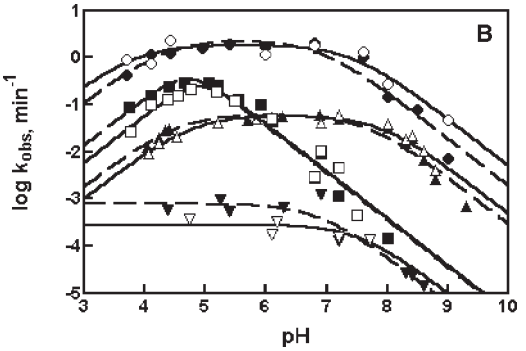

Figure 2. Continued

with the soman diastereomers yielded $pK_3 = 5.5$–5.8. Nearly symmetric pH curves, Fig. 2(B), for soman-inhibited wild-type and Glu197Asp Hu BChE gave $pK_2 = 3.7$–4.6 and $pK_3 = 7.3$–8.0, but much lower, $pK_3 \approx 5$, for the corresponding adduct of the Glu197Gln mutant. Dealkylation in soman-inhibited BChE is consistent with the participation of a carboxylic acid side-chain and $HisH^+438$. The p*K* of the Glu197Gln mutant drops significantly providing evidence for the negative charge on the carboxylate of Glu197 stabilizing $HisH^+438$, which is abolished in the neutral amide group. The already lower p*K* in Mo AChE adducts does not change. The unusually low p*K* of the catalytic His in ChEs has been the subject of much speculation.[26] Maximal rate constants for dealkylation are 1–6 min^{-1} for AChE and 2 min^{-1} for BChE at 25.0 °C.

pH-dependent reduction in the rate constants for dealkylation in the soman-inhibited mutants of AChEs and BChE[26]. The Glu202Gln mutation reduces the maximal rate constant for dealkylation 18-fold in the P(*S*)C(*S*)-soman-inhibited Mo AChE and 47-fold in the P(*S*)C(*R*)-soman-inhibited AChE adduct with respect to r Mo AChE at pH 5. The drop in the rate constant becomes equal, ~15-fold, between pH 5 and 9. The data published for the racemic soman-inhibited r Hu AChE, i.e. the reduction in the rate constant for dealkylation, is 260-fold at pH 6 and 137-fold at pH 8, giving a similar trend.[20] In contrast, the analogous comparison for *Tc* AChE gives a 17-fold rate reduction at pH 6 and 600-fold reduction at pH 8,[19] just the opposite of the two cases above. The p*K* of His440 has not been calculated from the pH dependence of the dealkylation reaction in soman-inhibited *Tc* AChE, but it may be higher than in the AChEs from other species and, thus, the decrease in this p*K* due to the removal of the stabilizing negative charge in Glu199 on $HisH^+$ 440 may have a more dramatic effect. Nonetheless, the case illustrates the caveat in drawing a simple general conclusion on the effect of the carboxylate group in Glu199 on dealkylation.

Table 2 provides a comparison of rate reductions, due to mutation in r Hu BChE, of the maximal rates, pH 5 or 6 [see Fig. 2(B)], and at pH 8.[26] The pH dependence of the effect of mutation is astonishing; the difference decreases for the Glu197Asp BChE when going from pH 5 to 8, which is similar to r Mo and Hu AChEs. However, the difference in the rate constants for dealkylation between soman-inhibited r and Glu197Gln BChE increases from pH 5 to 8, which is just the opposite of the other cases, but similar to *Tc* AChE. The Glu197Gln mutation reduces the p*K* of His438 in r Hu BChE by 3 units, which may also occur in the active-site milieu of native *Tc* AChE. The reduction in the rate of dealkylation in soman-inhibited Trp82Ala Hu BChE with respect to the native enzyme is 2500-fold in the adduct with the P(*S*)C(*S*) isomer of soman and 6000-fold in the adduct with the P(*S*)C(*R*) isomer of soman at pH 6. Similar observations were reported for r Hu AChE.[24] The mutation of Trp82 does

Table 1. Maximal rate constants (k_{max}) and p*K* values calculated for dealkylation in diastereomers of soman-inhibited cholinesterases[a]

Adduct, configuration of soman	k_{max} (min^{-1})	pK_1 (and pK_2)	pK_3	$k(H_2O)/k(D_2O)$
Mo AChE, P(*S*)C(*S*)	2.4 ± 0.5	4.5 ± 0.1	5.2 ± 0.2	1.3 ± 0.1
Mo AChE, P(*S*)C(*R*)	1.0 ± 0.1	4.1 ± 0.1	5.8 ± 0.1	
Mo AChE, E202Q P(*S*)C(*S*)	0.071 ± 0.008	—	5.8 ± 0.2	1.4 ± 0.2
Mo AChE, E202Q P(*S*)C(*R*)	0.021 ± 0.003	—	6.2 ± 0.2	
Hu BChE, P(*S*)C(*S*)[b]	2.0 ± 0.2	4.2 ± 0.1	7.5 ± 0.1	~1.3
Hu BChE, P(*S*)C(*R*)[b]	1.8 ± 0.4	3.7 ± 0.4	7.8 ± 0.4	
Hu BChE E197D, P(*S*)C(*S*)	0.056 ± 0.003	4.4 ± 0.1	8.0 ± 0.1	
Hu BChE E197D, P(*S*)C(*R*)	0.056 ± 0.003	4.7 ± 0.0	8.1 ± 0.1	
Hu BChE E197Q, P(*S*)C(*S*)	0.31 ± 0.03	4.6 ± 0.1	5.0 ± 0.1	
Hu BChE E197Q, P(*S*)C(*R*)	0.22 ± 0.03	4.9 ± 0.2	4.9 ± 0.2	
Hu BChE W82A, P(*S*)C(*S*)	0.0008 ± 0.0002	—	7.5 ± 0.6	
Hu BChE W82A, P(*S*)C(*R*)	0.0003 ± 0.0001	—	7.3 ± 0.4	
Ee AChE, P(*S*)C(*S*)[b]	6.3 ± 0.6	4.3 ± 0.1	6.0 ± 0.1	
Ee AChE, P(*S*)C(*R*)[b]	5.1 ± 0.4	4.3 ± 0.1	6.6 ± 0.2	
FBS AChE, P(*S*)C(*S*)[b]	3.1 ± 0.4	4.8 ± 0.1	5.0 ± 0.1	
FBS AChE, P(*S*)C(*R*)[b]	3.1 ± 0.4	4.8 ± 0.1	5.3 ± 0.1	

[a] Values calculated at $\mu = 0.1$ M (NaCl) and 25.0 ± 0.1 °C. Three-p*K* model; $pK_1 = pK_2$ for AChEs and two-p*K* model for BChE.
[b] Values are extrapolated from those measured at 4.0 ± 0.1 °C.

Table 2. Rate reduction, k_0/k, for dealkylation in soman-inhibited mutant r Hu BChEs

		k_0 (min^{-1})	k_0/k		
Inhibitor configuration	pH	Wild-type	E197D	E197Q	W82A
P(*S*)C(*S*)	5/6	2 ± 0.2	36 ± 5	6 ± 0.5	2500 ± 700
P(*S*)C(*S*)	8	0.18 ± 0.02	8 ± 2	450 ± 100	3200 ± 600
P(*S*)C(*R*)	5/6	1.8 ± 0.2	32 ± 5	8 ± 0.7	6000 ± 1000
P(*S*)C(*R*)	8	0.4 ± 0.05	14 ± 2	900 ± 100	6000 ± 1000

not change the pH dependence of the reaction since it does not involve a change in an ionizing group.

Stereoselectivity of dealkylation in soman-inhibited AChEs. Because of the difficulty in obtaining pure diastereomers of soman and the inefficiency of inhibiting ChEs with the P(*R*) diastereomers of soman, studies of the stereoselectivity of the aging reaction had to wait until fairly recently.[27] The selectivity for dealkylation is also 10^4-fold favoring the P(*S*) over the P(*R*) diastereomers in soman-inhibited r Hu AChE at pH 8.0 and 24.0 °C. This is fully consistent with the models presented above,[9,27] in which binding of the pinacolyl group at Trp84, Phe330 and Glu199 (and their equivalent in other ChEs) versus the acyl binding region accounts for the differences in propensity for promoting elimination of the pinacolyl group. Chirality at Cα has only a small effect on dealkylation in P(*S*)-soman-inhibited r Hu AChEs adducts. This is understandable by realizing that the position of the scissile C—O bond, with respect to residues interacting (or not) at the active site, cannot significantly change in spite the two different orientations of the small substituents around Cα. Moreover, the binding of methyl groups in Cβ to Trp84, Glu199 and Phe331 should also be very similar in the diastereomers to promote methyl migration equally. Mutations in r Hu AChE have a small effect on stereoselectivity of dealkylation, except for the Glu199Gln mutants, as shown above.

Solvent isotope effects. The other critical test of the mechanisms of acid–base-catalyzed reactions is solvent isotope effects.[38,39] The solvent isotope effects at the pH maxima are 1.3–1.4 indicating unlikely preprotonation or proton in 'flight' at the enzymic transition states.[26]

Small molecular products of the dealkylation in soman-inhibited ChEs. Product analysis of dealkylation in P(*S*)C(*S*)-soman inhibited Ee AChE[57] and r Hu BChE (C. Viragh, I. M. Kovach and A. Vertes, unpublished work) by GC–MS using selected ion monitoring mode has been carried out. The instrument was calibrated with pure standards of 2, 3-dimethyl-1-butene and 2,3-dimethyl-2-butene in the gas phase and methylene chloride extracts containing 2,3-dimethyl-2-butanol and 3,3-dimethyl-2-butanol in the aqueous phase. The dealkylation in soman-inhibited AChE at pH 5.0 ± 0.2 and 25.0 °C produces 40% alkenes and 50–60% 2,3-dimethyl-2-butanol. No 3,3-dimethyl-2-butanol could be detected to provide direct evidence of the intervention of a secondary carbenium ion on the reaction path. All products of the reaction originate from a tertiary carbenium ion. These results are in good agreement with the findings of Michel *et al.*[13]

Recent work in our group (J. Li and I. M. Kovach, unpublished work) targets appropriate non-enzymic cage complexes of phosphonate ester analogs of phosphonylated serine hydrolase enzymes that also undergo similar dealkylation reactions in an appropriate aqueous milieu. The molecular features incorporated into the host system are functional groups bearing high electron density. The enhancement of the rate of dealkylation in these systems are still below five orders of magnitude and seem to depend significantly on the orientation of the chiral Cα atom.

Species dependence and stereospecificity of dealkylation in soman-inhibited ChEs. Rate constants for dealkylation have been reported for a number of soman-inhibited cholinesterases,[11,13–15,19,20,26,58–60] but they have been measured at different pH, ionic strength and temperature. While this may impose some uncertainty in making comparisons, a summary of the data is provided in Table 3. The largest rate constants are for the Ee AChE. Dealkylation in soman-inhibited ChEs is an astonishing case of enzyme efficiency in catalyzing an evolutionarily unexpected reaction, quite unlike the natural reaction.

Molecular dynamics simulations of the tetracoordinate P(*S*)C(*S*)-soman-inhibited Tc AChE. The fully solvated tetracoordinate adduct formed between Ser200 Oγ of *Tc* AChE and soman was subjected to full-scale molecular dynamics simulation using CHARMM for >400 ps and compared with parallel simulations of the tetrahedral intermediate formed with the natural substrate acetylcholine.[44] Because the relevance of results of model calculations have always been a subject of debate,[24,27] the simulations included a water shell[61] and they were long enough to allow for equilibration of vibrational motions at least. A critical issue has been the protonation state of key catalytic residues. The orientation of flexible side-chains clearly depends on

Table 3. First-order rate constants for the dealkylation in soman-inhibited cholinesterases at the pH of maximal rate[m] or as reported

Source	k (min^{-1})	T (°C)	μ (M)	pH	Ref.
Ee AChE	4.8	25	0.84	5[m]	13
	1.0	25	0.84	7	13
	0.96	4	0.1	5[m]	11
	(6.3)[a]	(25)			
Tc AChE	0.34	25	0.064	6[m]	19
Muscles of plaice AChE	0.335	22	0.262	6.1	58
	0.071	22	0.064	7.4	58
r Mo AChE	1.2	25	0.1	5[m]	26
Rat brain AChE	0.26	37	0.064	7.3	60
FBS AChE	0.48	4	0.1	5[m]	11
	(3.1)[a]	(25)			
Bovine erythrocyte AChE	0.08	25	0.064	7.5	14
	0.115	25	0.064	7.4	60
	~0.7	5	0.155	5[m]	15
	(~5)[a]	(25)			
r Hu AChE	1.7	24	0.064	6[m]	20
r Hu BChE	0.22	4	0.1	6	26
	(2)[a]	(25)			

[a] Value extrapolated to 25 °C.

the choice of the assignment of protons to ionizing residues. X-ray structures of course are not very helpful guides in this regard, but experimental evidence or insight on p*K* values of groups and the pH at which experimental data are available for comparison should be taken into consideration. The protonation of His440 in covalent adducts of serine hydrolases has been well established (see above), and has been followed in all our calculations. The protonation state of carboxylic acids were the same as in the calculations of the McCammon group,[61] i.e. carboxylic acids except for Glu443 and Asp392, were unprotonated as assumed at physiological pH. Some simulations addressed the effect of protonation on Glu443, the results showed no perceptible influence on the conformation of Glu199. The pH dependence of substrate reactions with AChE, phosphonylation by soman, dealkylation of the soman-inhibited AChE and recent results of H NMR studies fully support our choices of protonation.

The simulations of the tetracoordinate adducts showed that NεH in $HisH^+$440 is not positioned to favor proton transfer to the pinacolyl O to promote its departure, whereas the optimized model confirmed the expected transfer of the proton from $HisH^+$440 to the O of the departing choline. In case of dealkylation, an electrostatic stabilization of the developing anion by $HisH^+$440 occurs. The alkyl fragment in the soman-inhibited adduct is destabilized by Trp84, Phe331 and Glu199, all within 3.7–3.9 Å from a methyl group in Cβ, 4.5–5.1 Å from Cβ and 4.8–5.8 Å from Cα. These residues are perfectly poised to promote methyl migration and stabilize electron deficiency in a developing carbenium ion in Cβ rather than in Cα. The same simulations were repeated with the Trp84Ala and Glu199Gln mutants of AChE. The Trp84Ala mutation eliminates interactions of the incipient carbenium ion with both the indole ring and benzene ring of Phe331 as well as Asp72, another key residue in catalytic action of AChE. The Glu199Gln (or Ala) mutations remove the charge of Glu199 and, thus, eliminate the electrostatic effect. Obviously, a Glu199Asp mutation also shortens the side-chain and, thereby, removes some of the interactions in which Glu199 engages. These mutations indeed reduced the rate of dealkylation significantly by 138–330-fold at pH 8.0 in r Hu AChE.[21,27] This effect is not at all 'indirect'[27] as limited stochastic boundary molecular mechanics calculations may suggest.[21,24] As outlined above, the unprotonated carboxyl side-chain of Glu199 engages in interactions with $HisH^+$440 and with the phosphonyl fragment in all of our calculations.

It was also revealed in our simulations that Tyr130 is likely to promote dealkylation by interacting with the indole ring of Trp84. The corresponding Trp86–Tyr133 interaction greatly affects phosphonylation and to a lesser extent dealkylation with soman inhibited r Hu AChE, based on studies with Tyr133Ala mutants.[27] Moreover, our simulations showed that Glu443 has an impact, via Tyr421, on the orientation of active-site residues Tyr442 and $HisH^+$440 in soman-inhibited AChE and, thus, this chain of interactions can also have a stabilizing effect on dealkylation. Shafferman's group recently reported a stabilizing effect of aromatic residues at the active site of r Hu AChE on the productive orientations of His447.[62]

High-resolution H NMR studies. The participation of Glu327 and Glu199 in the formation of tetracoordinate adducts has been further illuminated in our studies of low-field H NMR signals observed as short strong hydrogen bonds (SSHBs) form upon covalent modification of r Hu AChE[63] and equine (Eq) BChE[64] with phosphonate or

phosphate esters.[63–65] The His440 resonance at 14.4 ppm completely disappears in 3 h after addition of a 3-fold excess of 4-nitrophenyl-2-propyl methylphosphonate (a sarin analog) to a 0.1 mM (subunit) solution of Hu AChE at pH 7.5 and 25.0 °C. This is followed by a slower, $t_{1/2} = 13.2 \pm 5.7$ h at 25 °C, and simultaneous appearance of two peaks at 16.5 and 15.8 ppm, that grow to an integrated total area, which equals $97 \pm 10\%$ of the original signal. This rate is identical with that reported in a previous measurement of the rate of dealkylation in AChE phosphonylated by this inhibitor. The intensity ratio of the peaks for the 16.5/15.8 ppm resonances is 1.1 ± 0.1. Using an empirical correlation, H-bond lengths of 2.63 ± 0.02 and 2.65 ± 0.2 Å were calculated for the two slowly exchanging resonances at 16.5 and 15.8 ppm. The two bond lengths were also calculated from fractionation factor data, $\varphi = 0.47$ and 0.49 for the 16.5 and 15.8 ppm resonances, respectively, to obtain 2.55 ± 0.03 and 2.56 ± 0.03 Å, respectively. One of these SSHBs can be assigned to that formed between HisH$^+$440 Nδ and Glu327 Oε, as also observed in the x-ray structure of the methylphosphonate anion of the catalytic Ser of ChEs after dealkylation of either a soman or a sarin-inhibited ChE.[28] The second SSHB arises, most probably, from hydrogen bridging between HisH$^+$440 Nδ and Glu99 Oε, which is nearby. The x-ray structure does not confirm the latter, possibly because of species differences between homologous AChEs from Hu and *Tc*, or because the mixture of conformers may not form suitable crystals. It is, however, unlikely that the second SSHB would originate from either a hydrogen bridge between HisH$^+$440 and the anionic phosphonate oxygen or from steric effects, because two signals also emerge downfield concurrent with the disappearance of the 14.4 ppm signal when the pH is lowered and either r Hu AChE or Eq BChE is protonated.

Two downfield resonances were also found after inactivation of r Hu AChE with a 6-fold excess of 4-nitrophenyl bis-ethylphosphate (paraoxon). Again, the 14.4 ppm resonance completely disappears during data acquisition in ~3 h and a peak at 16.6 ppm and one at 15.5 ppm appear in a 1:2 ratio and in stoichiometric equivalence to the 14.4 ppm peak with a $t_{1/2} = 11 \pm 2$ days at 2.0 °C. The calculated lengths between H-bond donor and acceptor in these SSHBs are 2.63 ± 0.02 and 2.65 ± 0.02 Å and again are best assigned to conformational isomers, one in which the SSHB is between HisH$^+$440 Nδ and Glu327 Oε in the catalytic triad and the other is between HisH$^+$440 Nδ and Glu199 Oε. The ethylphosphate monoanion in this case is most certainly a product of an S_N2 type P—O bond cleavage as illustrated in Scheme 2.

The possibility of an SSHB between HisH$^+$440 and Glu199 may also be inferred from the x-ray structure of *O*-ethyl-*S*-{2-[bis(1-methylethyl)amino]ethyl} methylphosphonothioate (VX)-inhibited Hu AChE.[66] It is interesting that the ethyl methylphosphonate ester of Ser200

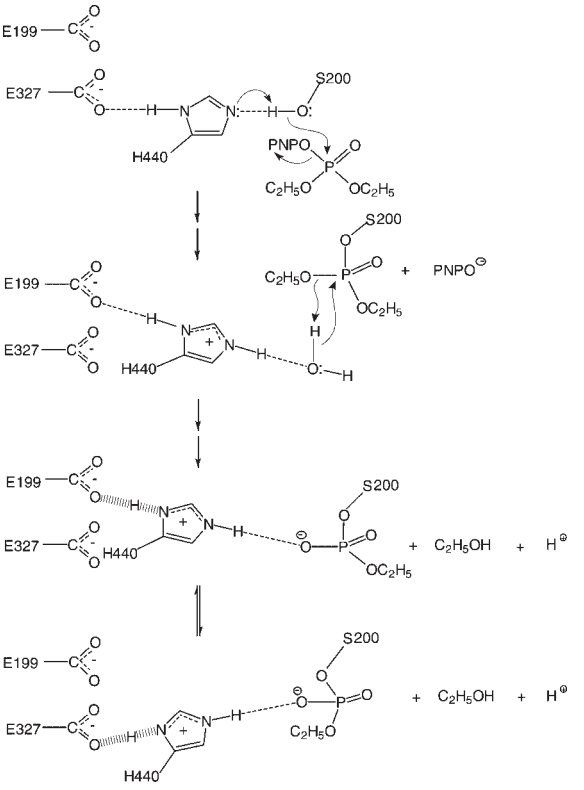

Scheme 2

in *Tc* AChE assumes the conformation in which HisH$^+$440 Nδ is 2.7 Å from Glu199 Oε and 4.5 Å from Glu327 Oε, while the more common or resting state conformation is observed for the native, reactivated and deethylated enzyme (presumable an S_N2 process).

A proton shuttling role of His in the catalytic triad was proposed by Jencks and co-workers,[67] then Bizozero and Dutler[68] based on physical organic reasoning: critical protonation of the poor leaving group is thus enforced. Calculations by Karplus and co-workers[69] with trypsin supported the possibility of an 'in' conformation of His195 in the tetrahedral adduct formed with 4-nitrophenyl acetate and an 'out' conformation in which HisH$^+$57 is poised for protonation of the leaving group. Our own calculations with the pentacoordinate P(*S*)C(*S*) and P(*S*)C(*R*) diastremeomers of soman-inhibited *Tc* AChE resulted in conformational differences in the optimized structures: the conformation observed with the pentacoordinate P(*S*)C(*S*)-soman-inhibited AChE adduct resembled the 'in' conformation of HisH$^+$440, while the P(*S*)C(*R*)-soman-inhibited AChE adduct seemed closer to the 'out' position of the catalytic HisH$^+$440.[8] It is worth noting that in contrast to the occurrence of the two downfield signals in H NMR and, thus, the conformational heterogeneity in phosphyl adducts of Hu AChE, none has been observed with Eq BChE, probably owing to the differences in active-site architecture. Also, only one downfield signal emerges when either Hu AChE or Eq BChE is inhibited with the transition-state analog TMTFA, confirming the observation with x-ray studies,

that Glu199 is engaged with the quaternary nitrogen of the adduct and, thus, is not available for forming an SSHB with His H^+440.[55] It may be remembered that the TMTFA adduct is an analog of the tetrahedral intermediate in acylation, which occurs before leaving group departure and is likely to have the 'in' conformation of the catalytic His440.

A self-consistent mechanism of dealkylation in soman-inhibited ChEs (Scheme 3)

The extensive pH profiles, solvent isotope effects and product distribution for the dealkylation reaction in soman-inhibited ChEs support the push–pull mechanism.[11,12,26,44,46–48] The essence of the mechanism is that the impetus for methyl migration stems from the electrostatic and steric push from the anionic binding site including Glu199 and Trp84 in the ground state. Concerted with methyl migration from Cβ to Cα, the C—O bond breaks without sharp charge polarization at the transition state and provides the soft interactions, which are the hallmark of enzyme catalysis.[36] $HisH^+440$ and the electropositive oxyanion hole provide the pulling effect to the C—O bond breaking and the ensuing development of the negative charge on the phosphonate monoester anion. This concerted transition structure may have nonclassical character. It appears that the enzyme stabilizes the transition state for dealkylation by $\sim 14\,\mathrm{kcal\,mol^{-1}}$ with respect to an appropriate nonenzymic reaction by avoiding the formation of at least one intermediate.[11] In the tertiary carbenium ion, the center of positive charge on the alkyl fragment is on Cβ, which is <4 Å from the N in the indole ring of Trp84, whereas Cα is ~ 7 Å from the same point, thus electrostatic stabilization by aromatic π electrons of the positive charge on Cβ is more substantial than on Cα.[44] The first intermediate formed is the tertiary carbenium ion, which then rapidly rearranges into neutral products. The catalytic function of Glu199 is apparently twofold: electrostatic in stabilizing the developing positive charge at the transition state for the formation of the tertiary carbenium ion and general base catalysis.

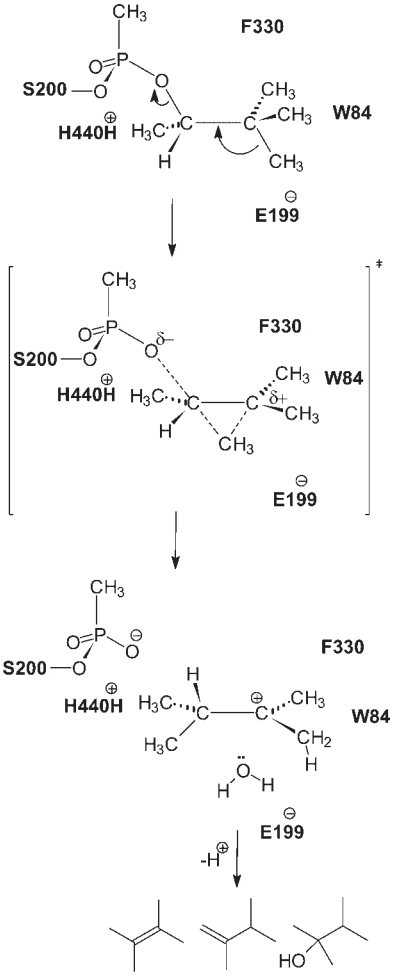

Scheme 3

The earlier (oxonium ion) mechanism[13,21–28] often cited is not consistent with the fact that (1) there were essentially no products isolated originating from the secondary cation, (2) rapid preprotonation followed by rate-determining formation of a secondary carbenium ion would be associated with an inverse solvent isotope effect, whereas the observed values are between 1.1 and 1.4 for the maximal rate constant for aging in soman-inhibited ChEs, and (3) the pH dependence of the reaction is consistent with pK values of the catalytic His in the phosphonate diester: 2 pK units higher in Hu BChE than in AChE. Differential calorimetric measurements for aged-soman-inhibited Hu BChE[70] and earlier structural investigations of serine proteases support a serine methylphosphonate anion–histidinium ion-pair product of dealkylation below pH $\sim$ 8–9.[50–54,71] (Note: x-ray data are consistent with these measurements; however, they do not provide information on the position of the proton.) This experimental fact is fully consistent with the thermodynamic preference for protonation of His, the stronger base of the two. Oxygen preprotonation in the pinacolyl group would then require a precise matching of the pKs at the transition state[67] of dealkylation and subsequent proton transfer back to His440 in the product state of the reaction. A concerted mechanism avoids this complexity.

Cation–π interactions between the incipient carbonium ion in aging phosphonylated adducts of Hu AChE and Trp86 have been championed by Shafferman's group.[20,21,24,27] They studied a homologous series of branched alkyl-chained phosphonate inhibitors and calculated the thermodynamic contribution of the degree of methyl substitution in Cβ to the efficiency of the reaction. Analogous studies were then carried out with the Trp86Phe and Trp86Ala mutants of Hu AChE. The stabilizing effect of Trp86 or Trp86Phe on the formation of the positive charge at Cα was attributed to cation–π

interactions only. Since then we observed a 265-fold rate reduction in the phosphonylation of Trp82Ala Hu BChE, which can only arise from elimination of simple binding to the 'wall' or conformational distortion because there is no cation occurring in these reaction. Thus, the elimination of the indole ring of Trp86 (or equivalent in other ChEs) elicits a complex effect on the rate of dealkylation, which includes a 10–100-fold reduction due to a loss of cation–π effects and a 16–265-fold reduction due to the loss of binding interactions or orientation effects of the indole ring. The dependence of activation energy differences for dealkylation between methyl-substituted and unsubstituted derivatives of alkyl methylphosphonyl adducts on the number of substitution were given in an apparent linear correlation;[27] however, the correlation alone does not lend confidence to a common mechanism. A progression of positive charge development in transition structures with increasing methyl substitution in Cβ, via changing mechanisms may be a more accurate view. Dealkylation in isopropyl side-chains of phosphonylated AChEs may not follow an S_N1 mechanism, while increasing methyl substitution will most likely promote the accumulation of positive charge on Cα, until trimethyl substitution results in methyl migration most likely concerted with C—O bond breaking, which spreads the charge to Cβ.

As our calculations also demonstrated, the Trp84Ala mutation causes changes in a number of interactions involving neighboring residues such as Phe331 and even an effect on the conformation of His440. The stabilizing effects of Trp84 and Glu199 are more likely to be on the delocalized (non-classical) carbenium ion with the center of the positive charge closer to Cβ than to Cα, formed during methyl migration.

Irreversible inhibition of serine proteases[49]

Chymotrypsin and trypsin react much slower with soman and phosphonate ester halides than the cholinesterases do. Dephosphonylation is also slower in serine proteases.[72] There is slow dealkylation in soman-inhibited chymotrypsin and trypsin, but it is not the S_N1 type.[11] This is in spite of the presence of Trp215 in the specificity pocket; however, the binding of the pinacolyl group in the diastereomers of soman has not been studied.

In contrast, chymotrypsin, trypsin and subtilisin BPN′ can be effectively inhibited by 4-nitrophenyl phosphonate esters. The inactivation of chymotrypsin and subtilisin BPN′ by bis-4-nitrophenyl methylphosphonate (NMN) and bis-4-nitrophenyl propylphosphonate (NPN) give second-order rate constants, k_i/K_i, between 544 and $4300\,\text{M}^{-1}\,\text{s}^{-1}$ at $25.0 \pm 0.1\,^{\circ}\text{C}$ at the pH maxima. The second-order rate constants for the inhibition of trypsin are $26.3 \pm 1.4\,\text{M}^{-1}\,\text{s}^{-1}$ with NMN and $891 \pm 14\,\text{M}^{-1}\,\text{s}^{-1}$ with NPN at pH 8.3 and $25.0 \pm 0.1\,^{\circ}\text{C}$. A second stoichiometric equivalent 4-nitrophenol is also lost from 4-nitrophenyl alkylphosphonyl adducts of chymotrypsin but not from trypsin and subtilisin BPN′. Elimination of 4-nitrophenol from the propylphosphonyl adduct is at a rate only about twice the rate of hydrolysis of a comparable phosphonate diester, whereas 4-nitrophenol is eliminated 270 times faster from the methylphosphonyl adduct of chymotrypsin. The activation enthalpies, in kcal mol^{-1}, for 4-nitrophenol elimination from 4-nitrophenyl alkylphosphonyl-chymotrypsin are 15.0 ± 1.3 for the propyl derivative, 16.4 ± 0.5 for the methyl derivative in H_2O and 18.0 ± 0.5 in D_2O. The activation entropies, in $\text{cal mol}^{-1}\,\text{K}^{-1}$, are -29.7 ± 2.4 for the propyl derivative, -14.8 ± 0.5 for the methyl derivative in H_2O and -10.3 ± 0.3 in D_2O. Partial solvent isotope effects for the elimination of 4-nitrophenol from 4-nitrophenyl methylphosphonyl-chymotrypsin give best fits to two-site proton models (Fig. 3): these give primary isotope effects between 1.9 and 2.0 ($\varphi_1^{\ddagger} = 0.52 \pm 0.14$ or 0.49 ± 0.07) for a proton in flight, possibly from the water attacking at phosphorus to the catalytic His, and an α-secondary effect of 1.3 ($\varphi_2^{\ddagger} = 0.75 \pm 0.20$) or a term for solvent contribution of 1.25 ($\Phi = 0.80 \pm 0.10$). The secondary β-deuterium isotope effect on the elimination of the second 4-nitrophenol from the adduct of chymotrypsin with NMN-l_3 (l = h or d) is 0.94 ± 0.2 possibly due to hyperconjugation. Scheme 4 shows the mechanism of general base-catalyzed P—O bond cleavage that the kinetic data support.

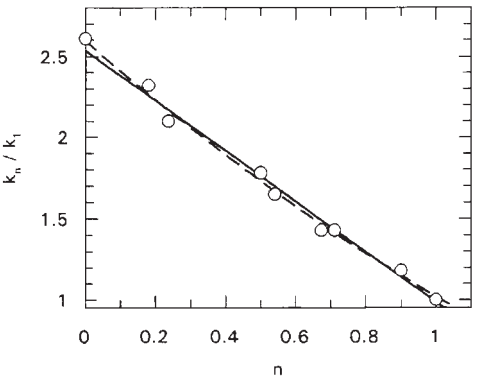

Figure 3. Partial solvent isotope effects (k_n/k_1) as a function of atom fraction deuterium (n) for 4-nitrophenol release from the adduct of chymotrypsin with NMN. The symbols represent ratios, within one standard deviation, of the average of at least three rate constants, the heavy line is the best linear least-squares fit of the data $k_n/k_1 = 2.54(1 - n + 0.39)$ and the dashed line is the non-linear least-squares fit of the data to either $k_n/k_1 = 2.60(1 - n + 0.52n)(1 - n + 0.75n)$ or $k_n/k_1 = 2.60(1 - n + 0.49n)(0.8n)$

CONCLUSIONS

The efficiency of phosphonylation of serine hydrolase enzymes depends on the exploitation by the inhibitors of the enzyme characteristics that dictate specificity and

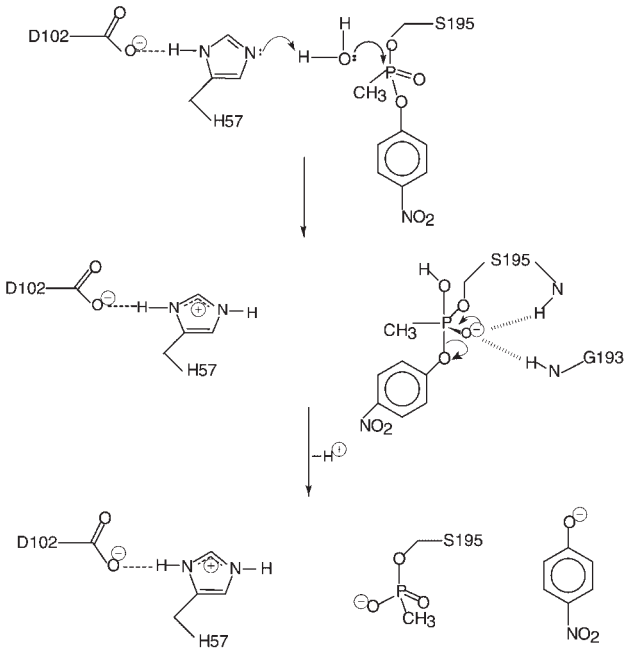

Scheme 4

efficient binding of the substrate. In ChEs, where substrate binding does not involve as many specific interactions as in serine proteases, enzyme active-site features (Trp84, Glu199, Phe331) exist to promote exceptionally efficient departure of an F^- leaving group. The acyl-binding site, available for pinacolyl in the P(*R*) diastereomers of soman, is four orders of magnitude less accommodating.

The mechanisms of secondary reactions from phosphonylated serine protease enzymes are markedly different from ChEs. The most obvious differences between the active-site architecture of the two groups of serine hydrolase enzymes are the open well-solvated funnel-type active site in serine proteases versus a deep hydrophobic gorge in AChEs. BChEs also have the long hydrophobic gorge, but the active site is more spacious and contains more aliphatic side-chains.[42] The uniquely efficient dealkylation reaction observed in P(*S*)-soman-inhibited AChEs seems to originate from a combination of the presence of an assembly of residues cooperatively promoting methyl migration and stabilizing the development of positive charge in a generally hydrophobic environment.

Phosphylation and dephosphylation are frequently compared with the nucleophilic double displacement, which is the hallmark of serine hydrolase function. Dealkylation in soman-inhibited ChEs, in contrast, occurs with the loss of electrons in the reacting fragment and transfer of electrons to the enzyme active site. ChEs having high electron density at their active site in the native state and neutral pH further enhance their electron density by covalently binding a negatively charged fragment at the end of the reaction. The electrostatic catalysis initiating the push–pull action of the enzyme results in the departure of neutral products and leaves enhanced electron density at the catalytic site.

Acknowledgments

This work was supported in part by DAMD17-C-98-8021, DAAH04-96-C-0086, USAMRICD NSF MCB9205927 and NIH Research Fellowship 1 F33 AG05742-01. The contributions of Dr Carol Viragh deserve special recognition. The author expresses gratitude to all collaborators in Refs 4, 6, 8–12, 26, 29–36, 44, 49, 57 and 63–65.

REFERENCES

1. Bourne N, Williams A. *J. Am. Chem. Soc.* 1984; **106**: 7591–7596.
2. Kovach IM. *J. Enzyme Inhib.* 1988; **2**: 199–208.
3. Jencks WP. *Catalysis in Chemistry and Enzymology*. McGraw-Hill: New York, 1969 (Dover edition, 1987).
4. (a) Qian NF, Kovach IM. *Med. Defense Biosci. Rev.* 1993; **3**: 1005–1014; (b) Qian N, Kovach IM. *FEBS Lett.* 1993; **336**: 263–266.
5. (a) Kovach IM. *Phosphorus Sulfur Silicon* 1993; **75**: 131–134; (b) Kovach IM. *J. Enzyme Inhib.* 1991; **4**: 201–212.
6. Bencsura A, Enyedy I, Viragh C, Akhmetshin R, Kovach IM. In *Enzymes of the Cholinesterase Family*, Quinn DM, Balasubramanian AS, Doctor BP, Taylor P (eds). Plenum Press: New York, 1995; 155–162.
7. Kovach IM. *THEOCHEM* 1988; **47**: 159–169.
8. Bencsura A, Enyedy I, Kovach IM. *Biochemistry* 1995; **34**: 8989–8999.
9. Bencsura A, Enyedy I, Kovach IM. *J. Am. Chem. Soc.* 1996; **118**: 8531–8541.
10. Enyedy I, Bencsura A, Kovach IM. *Phosphorus Sulfur Silicon* 1996; **109–110**: 249–252.
11. Viragh C, Akhmetshin R, Kovach IM, Broomfield C. *Biochemistry* 1997; **36**: 8243–8252.
12. Kovach IM, Akhmetshin R, Enyedy IJ, Viragh C. *Biochem J.* 1997; **324**: 995–996.
13. Michel HO, Hackley BE, Berkowitz L, List G, Gillian W, Pankau M. *Arch. Biochem. Biophys.* 1967; **121**: 29–34.
14. Keijer JH, Wolring GZ. *Biochim. Biophys. Acta* 1969; **185**: 465–468.
15. Schoene K, Steinhanses, Wertman A. *Biochim. Biophys. Acta* 1980; **616**: 384–388.
16. Benschop HP, Konings CA, VanGenderen J, DeJong LP. *Toxicol. Appl. Pharmacol.* 1984; **72**: 61–74.
17. Sun MC, Li FZ, Chou TC. *Biochem. Pharmacol.* 1986; **35**: 347–349.
18. (a) Segall Y, Waysbort D, Barak D, Ariel N, Doctor BP, Grunwald J, Ashani Y. *Biochemistry* 1993; **32**: 13441–13450; (b) Steinberg N, van der Drift ACM, Grunwald J, Segall Y, Shirin E, Haas E, Ashani Y, Silman I. *Biochemistry* 1989; **28**: 1248–1254.
19. Saxena A, Doctor BP, Maxwell DM, Lenz DE, Radic Z, Taylor P. *Biochem. Biophys. Res. Commun.* 1993; **197**: 343–349.
20. Ordentlich A, Kronman C, Barak D, Stein D, Ariel N, Marcus D, Velan B, Shafferman A. *FEBS Lett.* 1993; **334**: 215–220.
21. Shafferman A, Ordentlich A, Barak D, Stein D, Ariel N, Velan B. *Biochem. J.* 1996; **318**: 833–840.
22. Shafferman A, Ordentlich A, Barak D, Stein N, Ariel N, Velan B. *Biochem. J.* 1997; **324**: 996–998.
23. Saxena A, Maxwell DM, Quinn DM, Radic Z, Taylor P, Doctor BP. *Biochem. Pharmacol.* 1997; **54**: 269–274.
24. Barak D, Ordentlich A, Segall Y, Velan B, Benschop HP, DeJong LP, Shafferman A. *J. Am. Chem. Soc.* 1997; **119**: 3157–3158.
25. Masson P, Fortier P, Albaret C, Froment MT, Bartels CF, Lockridge O. *Biochem. J.* 1997; **327**: 601–607.
26. Saxena A, Viragh C, Frazier DS, Kovach IM, Maxwell DM, Lockridge O, Doctor BP. *Biochemistry* 1998; **37**: 15086–15096.

27. Ordentlich A, Barak D, Kronman C, Benchop HP, De Jong LPA, Ariel N, Barak R, Segall Y, Velan B, Shafferman A. *Biochemistry* 1999; **38**: 3055–3066.
28. (a) Millard CB, Kryger G, Ordentlich A, Greenblatt HM, Harel M, Raves ML, Segall Y, Barak D, Shafferman A, Silman I, Sussman JL. *Biochemistry* 1999; **38**: 7032–7039; (b) Millard CB, Kryger GO, Harel M, Raves ML, Greenblat H, Segall Y, Barak D, Shafferman A, Silman I, Sussman JL. In *Structure and Function of Cholinesterases and Related Proteins*, Doctor BP, Quinn DM, Rotundo RL, Taylor P (eds). Plenum Press: London, 1998; 425–431.
29. Kovach IM, Huhta D. *THEOCHEM* 1991; **79**: 335–342.
30. Kovach IM, Schowen RL. In *Peptides and Proteases: Recent Advances*, Schowen RL, Barth A (eds). Pergamon Press: Oxford, 1987; 205–205.
31. Kovach IM, Larson M, Schowen RL. *J. Am. Chem. Soc.* 1986; **108**: 5490–5495.
32. Kovach IM, Huber-Ashley H, Schowen RL. *J. Am. Chem. Soc.* 1988; **110**: 590–593.
33. Bennet AJ, Kovach IM, Schowen RL. *Pestic. Biochem. Physiol.* 1989; **33**: 78–82.
34. Bennet A, Kovach IM, Schowen RL. *J. Am. Chem. Soc.* 1988; **110**: 7892–7893.
35. Bennet AJ, Kovach IM, Bibbs JA. *J. Am. Chem. Soc.* 1989; **111**: 6424–6427.
36. Kovach IM, Bennet AJ. *Phosphorus Sulfur Silicon* 1990; **51/52**: 51–56.
37. Fersht A. *Structure and Mechanism in Protein Science*. Freeman: New York, 1999; 169–188, 472–486.
38. (a) Schowen RL. In *Transition States of Biochemical Processes*, Gandour RD, Schowen RL (eds). Plenum Press: New York, 1978; 77–113; (b) Alvarez FJ, Schowen RL. In *Isotopes in Organic Chemistry*, Buncel E, Lee CC (eds). Elsevier: Amsterdam, 1987; 1–60.
39. Quinn MD, Sutton LD. In *Enzyme Mechanisms from Isotope Effects*, Cook PF (ed). CRC Press: Boston, 1991; 73.
40. (a) Broomfield CA, Millard CB, Lockridge O, Caviston TL. In *Enzymes of the Cholinesterase Family*, Quinn DM, Balasubramanian AS, Doctor BP, Taylor P (eds). Plenum Press: New York, 1995; 169–175; (b) Millard CB, Lockridge O, Broomfield CA. *Biochemistry* 1998; **37**: 237–247; (c) Lockridge O, Blong RM, Masson P, Froment MT, Millard CB, Broomfield CA. *Biochemistry* 1997; **36**: 786–795.
41. Sussman JL, Harel M, Frolow F, Oefner C, Goldman A, Toker L, Silman I. *Science* 1991; **253**: 872–879.
42. (a) Taylor P, Radic Z. *Annu. Rev. Pharmacol. Toxicol*. 1994; **34**: 281–320; (b) Radic Z, Gibney G, Kawamoto S, MacPhee-Quigley K, Bongiorno C, Taylor P. *Biochemistry* 1992; **31**: 9760–9767; (c) Kovarik Z, Radic Z, Berman HA, Simeon-Rudolf V, Reiner E, Taylor P. *Biochem J.* 2003; **373**: 33–40.
43. (a) Schrag JD, Li Y, Wu S, Cygler M. *Nature* 1991; **351**: 761–764. (b) Brozowski AM, Derewenda U, Derewenda ZS, Dodson GG, Lawson DM, Turkenburg JP, Bjorkling F, Huge-Jenses B, Patkar SA, Thim L. *Nature* 1991; **351**: 491–494.
44. Enyedy IJ, Kovach IM, Bencsura A. *J. Biochem.* 2001; **353**: 645–653.
45. (a) De Jong LP, Wolring GZ. *Biochem. Pharmacol.* 1988; **33**: 1119–1125; (b) De Jong LPA, Benchop HP. In *Stereoselectivity of Pesiticides: Biological and Chemical Problems*, Arien EJ, van Rensen JJS, Welling W (eds). Elsevier: Amsterdam, 1988; 109–149.
46. Kovach IM. *Phosphorus Sulfur Silicon* 1999; **144–146**: 537–540.
47. Kovach IM. *Biokemia* 2001; **25**: 74–80.
48. Kovach IM. In *Structure and Function of Cholinesterases and Related Proteins*, Doctor BP, Taylor P, Quinn DM, Rotundo RL, Gentry MK (eds). Plenum Press: New York, 1998; 339–344.
49. Kovach IM, Enyedy EJ. *J. Am. Chem. Soc*. 1998; **120**: 258–263.
50. Kossiakoff AA, Spencer SA. *Biochemistry* 1981; **20**: 6462–6474.
51. Porubcan MA, Westler WM, Ibanez IB, Markley JL. *Biochemistry* 1979; **18**: 4108–4116.
52. Jordan F, Polgar L, Tous G. *Biochemistry* 1985; **24**: 7711–7717.
53. Frey PA, Whitt SA, Tobin JB. *Science* 1994; **264**: 1927–1930.
54. Cassidy CS, Lin J, Frey PA. *Biochemistry* 1997; **36**: 4576–4584.
55. Harel M, Quinn DM, Nair HK, Silman I, Sussman JL. *J. Am. Chem. Soc*. 1996; **118**: 2340–2346.
56. Selwood T, Feaster SR, States MJ, Pryor AN, Quinn DM. *J. Am. Chem. Soc*. 1993; **115**: 10477–10482.
57. Viragh C, Kovach IM, Pannell L. *Biochemistry* 1999; **38**: 9557–9561.
58. Bucht G, Puu G. *Biochem. Pharmacol.* 1984; **33**: 3573–3577.
59. Fleisher JH, Harris LW. *Biochem. Pharmacol.* 1965; **14**: 641–650.
60. Coult DB, Marsh DJ, Read G. *Biochem. J.* 1965; **98**: 869–873.
61. (a) Gilson MK, Straasma TP, McCammon JA, Ripoll DR, Faerman CH, Axelsen PH, Silman I, Sussman JL. *Science* 1994; **263**: 1276–1278; (b) Wlodeck ST, Clark TW, Scott LR, McCammon JA. *J. Am. Chem. Soc.* 1997; **119**: 9513–9522.
62. Barak D, Kaplan D, Ordentlich A, Ariel N, Velan B, Shafferman A. *Biochemistry* 2002; **41**: 8245–8254.
63. Massiah MA, Viragh C, Reddy PM, Kovach IM, Johnson J, Rosenberry TL, Mildvan AS. *Biochemistry* 2001; **40**: 5682–5690.
64. Viragh C, Harris TK, Massiah MA, Mildvan AS, Kovach IM. *Biochemistry* 2000; **39**: 16200–16205.
65. Mildvan AS, Massiah MA, Harris TK, Marks G, Harrison DHT, Viragh C, Reddy PM, Kovach IM. *J. Mol. Struct.* 2002; **615**: 163–175.
66. Millard CB, Koellner G, Ordentlich A, Shafferman A, Silman I, Sussman JL. *J. Am. Chem. Soc.* 1999; **121**: 9883–9884.
67. (a) Satterwhait AC, Jencks WP. *J. Am. Chem Soc.* 1974; **96**: 7018–7031; (b) Jencks WP. *Adv. Enzymol. Relat. Areas Mol. Biol.* 1975; **43**: 219–410.
68. Bizozero SA, Dutler H. *Bioorg. Chem.* 1981; **10**: 46–55.
69. Nakagawa S, Yu H, Karplus M, Umeyama H. *Proteins: Struct. Funct. Genet*. 1993; **16**: 172–194.
70. Masson P. *Biochem. J.* 1999; **343**: 361–369.
71. Bachovchin WW. *Biochemistry* 1986; **25**: 7751–7759.
72. Hovanec JW, Lieske CN. *Biochemistry* 1972; **6**: 1051–1058.